Genes & Diseases (2023) 10, 1582–1595

Available online at www.sciencedirect.com

ScienceDirect

journal homepage: www.keaipublishing.com/en/journals/genes-diseases

FULL LENGTH ARTICLE

Progranulin regulation of autophagy contributes to its chondroprotective effect in osteoarthritis

Yiming Pan [a,1], Yuyou Yang [a,1], Mengtian Fan [a], Cheng Chen [b], Rong Jiang [c], Li Liang [a], Menglin Xian [a], Biao Kuang [d], Nana Geng [a], Naibo Feng [a], Lin Deng [a], Wei Zheng [a], Fengmei Zhang [e], Xiaoli Li [a], Fengjin Guo [a,*]

[a] *Department of Cell Biology and Genetics, Core Facility of Development Biology, Chongqing Medical University, Chongqing 400016, China*
[b] *Department of Orthopaedics, The 1st Affiliated Hospital of Chongqing Medical University, Chongqing 400016, China*
[c] *Laboratory of Stem Cells and Tissue Engineering, Chongqing Medical University, Chongqing 400016, China*
[d] *Department of Orthopaedics, The 2nd Affiliated Hospital of Chongqing Medical University, Chongqing 400016, China*
[e] *Chongqing Medical University Laboratory Animal Center, Chongqing Medical University, Chongqing 400016, China*

Received 27 January 2022; received in revised form 3 May 2022; accepted 21 May 2022
Available online 13 June 2022

KEYWORDS
Anabolism;
ATG12;
ATG5;
Autophagy;
Catabolism;
Osteoarthritis;
PGRN

Abstract Progranulin (PGRN) is a multifunctional growth factor involved in many physiological processes and disease states. The apparent protective role of PGRN and the importance of chondrocyte autophagic function in the progression of osteoarthritis (OA) led us to investigate the role of PGRN in the regulation of chondrocyte autophagy. PGRN knockout chondrocytes exhibited a deficient autophagic response with limited induction following rapamycin, serum starvation, and IL-1β-induced autophagy. PGRN-mediated anabolism and suppression of IL-1β-induced catabolism were largely abrogated in the presence of the BafA1 autophagy inhibitor. Mechanistically, during the process of OA, PGRN and the ATG5–ATG12 conjugate form a protein complex; PGRN regulates autophagy in chondrocytes and OA through, at least partially, the interactions between PGRN and the ATG5–ATG12 conjugate. Furthermore, the ATG5–ATG12 conjugate is critical for cell proliferation and apoptosis. Knockdown or knockout

* Corresponding author.
E-mail addresses: guo.fengjin@gmail.com, guo.fengjin@cqmu.edu.cn (F. Guo).
Peer review under responsibility of Chongqing Medical University.
[1] These authors contributed equally to this work.

https://doi.org/10.1016/j.gendis.2022.05.031

of ATG5 reduces the expression of ATG5—ATG12 conjugate and inhibits the chondroprotective effect of PGRN on anabolism and catabolism. Overexpression of PGRN partially reversed this effect. In brief, the PGRN-mediated regulation of chondrocyte autophagy plays a key role in the chondroprotective role of PGRN in OA. Such studies provide new insights into the pathogenesis of OA and PGRN-associated autophagy in chondrocyte homeostasis.

Introduction

Osteoarthritis (OA), a common chronic degenerative disease, has attracted increasing attention in the last decades. OA involves the destruction of articular cartilage and sclerosis or causticization of subchondral bone, osteophyte formation, and chronic inflammation of the synovium. Many factors have been reported to participate in the pathogenesis of OA, including hereditary, mechanical, and aging-related factors; however, the specific role of these factors in OA remains unclear, and the pathogenesis of OA has not been fully understood.[1,2] The occurrence and development of OA and the pathological changes in articular cartilage have been reported to be closely associated with autophagy, which includes 4 stages: initiation, elongation, maturation, and termination. Abnormalities in each stage of autophagy have been found to be involved in different stages of OA development.[3,4] Lotz M. et al reported that autophagy was inhibited in human OA cartilage as well as in the cartilage of mouse OA models, and this reduction was accompanied by an enhancement in cell apoptosis.[5] In the process of autophagy, a variety of autophagy related (ATG) proteins are recruited to phagocytes to form autophagosomes. ATG12 is activated by ATG7 and then binds to ATG5 under the action of ATG10. One of the functions of the ATG12-ATG5 conjugate is to promote the lipidation of LC3.[6]

Aging or excessive mechanical load on articular cartilage is known to lead to significant damage to chondrocytes and the extracellular matrix. Importantly, autophagy induction has not only been shown to protect against cell death and maintain cell homeostasis, it is also known to reduce the loss of group-specific antigens after mechanical injury and aging. Many studies have reported the constitutive activation of autophagy, thus regarding it as a protective or homeostatic mechanism of normal cartilage.[5,7,8] Autophagy is involved in the pathogenesis of OA through the modulation of chondrocyte homeostasis. Loss of autophagy has been associated with pathological changes in OA.[9,10]

Progranulin (PGRN) is a widely expressed growth factor with multiple functions that participate in anti-inflammatory and anti-infection processes, host defense, cartilage development, wound healing, and tissue repair.[11] PGRN was previously reported to be upregulated in OA, and it significantly attenuated OA-like phenotypes and protected against OA progression through its action in chondrocyte metabolism.[1,12] PGRN, as an antagonist of the TNFa signaling, was found to play a vital role in the pathogenesis of inflammatory arthritis in mice.[2,13] More interestingly, intracellular PGRN was shown to regulate autophagy and lysosome integrity in macrophages; PGRN deficiency reportedly caused autophagy defects in macrophages, resulting in lysosomal storage diseases.[1,14,15] These previous reports prompted us to determine whether PGRN regulates chondrocyte autophagy and whether the PGRN-mediated regulation of autophagy is important for the protective role of PGRN in OA.

This study identified that PGRN serves as an essential mediator of autophagy activation *in vitro* and *in vivo* and PGRN-mediated autophagy is essential for its chondroprotective effect in OA. Importantly, we found that the mechanism by which PGRN might regulate chondrocyte autophagy could be through interactions between the PGRN and the ATG5-ATG12 conjugate.

Materials and methods

Human tissue collection

Human cartilage samples were collected from patients with OA. Human joint tissues were collected from OA patients undergoing knee replacement surgery from The First Affiliated Hospital of Chongqing Medical University and The Second Affiliated Hospital of Chongqing Medical University. They were taken out during the operation with the consent of the patients, and then stored in liquid nitrogen for standby. The damaged cartilage and the undamaged cartilage were isolated from OA joint respectively. The damaged articular cartilage within 2—3 mm of the macroscopic OA lesion was surgically removed and collected, meanwhile, the undamaged cartilage was isolated from adjacent non-lesion cartilage of the femoral condyle considered by the surgeon to look like intact and healthy cartilage.[16—19] The same sample source can reduce the impact of different genetic backgrounds. Furthermore, in order to ensure accurate separation of tissues, we also detected mRNA level of some typical cartilage metabolism marker genes, including Col2, Aggrecan and MMP13, in the damaged cartilage and the undamaged cartilage tissues. The QPCR results proved that our isolation of damaged and undamaged cartilage tissues was accurate. A total of 14 samples were collected for western blotting and qPCR, including 8 damaged OA cartilage tissue and 6 undamaged cartilage tissue. All biomedical studies involving humans in this study were reviewed and approved by the Ethics Committee of Chongqing Medical University.

Mice and surgically induced osteoarthritis mice model

All animal studies were performed in accordance with the Institutional guidelines and approval by the Chongqing Medical University Institutional Animal Care and Use Committee. 6 6-month-old male C57BL/6J mice were randomly assigned to each group according to the method of random number table. All animals were maintained on a 12-h light—dark cycle in a rodent barrier facility at the animal house of Chongqing Medical University with adlibitum access to water and food throughout the study. Genotyping of *GRN*-knockout ($GRN^{-/-}$) and wild-type (WT) litter mates was performed as previously described[20,21] (Fig. S1).

Destabilization of the medial meniscus (DMM) surgery was performed in the right hind limbs of age-matched mice in accordance with previous reports.[22–25] Six-month-old WT and $GRN^{-/-}$ (*PGRN* KO) mice were subjected to DMM surgery. In short, first, under anesthesia, a 3 mm longitudinal incision was made on the medial side of the knee joint to passively separate the knee extensor and patellar ligament, and expose the medial meniscus ligament (MMTL). Then the MMTL was transected to make the DMM unstable. Finally, suture the medial joint capsule and close the skin. As a control, sham operation was performed on the left knee joint with medial capsulotomy only. To investigate the effect of recombinant PGRN (rhPGRN) and Baf A1, 6-month-old WT and PGRN KO mice were subjected to DMM surgery followed by intra-articular injection of phosphate buffered saline (PBS) and rhPGRN (6 μg) with or without Baf A1 (5 μg) for 4 weeks. Six mice were used for each time point in each treatment group. Animals were sacrificed at 4, 8, or 12 weeks after intra-articular injection respectively. For DMM model group, 6 mice refer to mice with OA after successful DMM operation.

Protein and RNA detection

Every (10—20) mg of joint tissue or (2—5) $\times$ 10^6 cells were used as a reaction dose. Protein extracts and separated by 10% SDS-PAGE. Proteins were subsequently transferred to a PVDF membrane (Millipore) and blocked for 2 h in 5% nonfat dry milk. Membranes were then incubated with primary antibodies at 4 °C overnight, and then incubated with secondary antibody for 2 h. GAPDH is which widely distributed in various tissues and cells with high levels. GAPDH and β-actin are widely distributed in various tissues and cells with high levels. The amount of GAPDH or β-actin expression in the same cell or tissue is generally constant and is rarely affected by external inducers. However, the presence of diseases such as hypoxia and diabetes will affect the expression of GAPDH. Instead of hypoxia, we used rapamycin to induce autophagy. Similarly, in the study of chondrocyte autophagy induced by rapamycin, some scholars chose GAPDH as the reference gene,[26–28] in addition, the molecular weight difference between the target protein and GAPDH or β-actin in this article is at least 5kD, which is convenient for the analysis of the results, so GAPDH were used as reference gene.

qPCR was performed to examine changes in target genes. Briefly, 20 mg cartilage or 2 $\times$ 10^6 cells were harvest for RNA extraction. Total RNA was extracted using FastPure® Cell/Tissue Total RNA Isolation Kit (Vazyme Biotech, RC101) and cDNA was immediately synthesized from total RNA (1 μg) using the HiScript® II Q RT SuperMix for qPCR (+gDNA wiper) (Vazyme Biotech, R223- 01). qPCR was carried out on CFX Connect™ Real-Time PCR Detection System (Bio-Rad Laboratories, Inc.) using ChamQ Universal SYBR qPCR Master Mix (Vazyme Biotech, Q711) according to the following protocol: preheating at 95 °C for 30 s, 40 cycles at 95 °C for 10 s and 58 °C for 30 s, and then a dissociation curve performed at 95 °C for 15 s, 60 °C for 60 s, and 95 °C for 15 s. GAPDH was used as an internal control gene. Primer information is shown in Supplementary Information of Primers were synthesized by Tsingke (Tsingke Biotechnology Co., Ltd., China) were showed in Table S1. The target genes were quantified using the comparative threshold cycle (Ct) values $2^{-\Delta\Delta Ct}$ method ($\triangle$ Ct = CtTarget gene − CtGAPDH, $\triangle\triangle$ Ct = $\triangle$ CtTreatment − $\triangle$ CtControl). Experiments were repeated three times.

Construction of pSES-HUS-ATG5 siRNA recombinant adenovirus shuttle plasmid

Use Oligoengine software to design the ATG5 interference siRNA sequence online, and select a relatively high inhibitory sequence for synthesis (Table S2). The SfiI linearized pSES-HUS plasmid and the annealed ATG5 siRNA interference sequence were T4 ligated, and the adenovirus plasmid Ad-ATG5 siRNA was constructed by homologous recombination by electroporation.

Immunofluorescence assay and transmission electron microscope (TEM)

Cells were incubated with first antibodies (1:100) at 4 °C overnight, and then incubated with fluorescence-labeled secondary antibodies at 4 °C for 1 h. Fluorescence intensities were quantified using the ImageJ software. Different autophagy-related ultrastructure was determined under a Philips CM-12 electron microscope (FEI; Eindhoven, Netherlands) and photographed with a Gatan (4 k $\times$ 2.7 k) digital camera (Gatan, Inc., Pleasanton, CA, USA). The pictures taken are counted using the methods recommended by the Autophagy Guidelines.[29]

Knockout of *GRN* and *ATG5* gene in chondrocytes using the CRISPR-Cas9 technique

Knockout of *GRN* and *ATG5* gene of C28/I2 human chondrocytes was generated in accordance with a previously published protocol.[30,31]shRNA targeting *GRN* was inserted into the lentiCRISPR V2 vector (Addgene). The vector was packaged into lentiviruses by cotransfecting with lentiCRISPR V2, VSVG5, and CMV in HEK293T cells. After packaging, C28/I2 chondrocytes were infected with lentiviruses collected over 8 h. Puromycin (2 μg/mL) was used to select stably transfected C28/I2 cells. $ATG5^{-/-}$ chondrocytes were also generated using the CRISPR-Cas9 technique, similar to this method. Puromycin (2 μg/mL) was used to select stably transfected C28/I2 cells. The specific *GRN*-knockout and *ATG5*-knockout primer pairs were showed in Table S3 of Supplementary Materials.

Cultivation of mouse cartilage explants and primary articular chondrocytes

Cartilage explants from humans and mice were cultured in the same way as previously reported.[32–34] Murine articular chondrocytes were isolated from the articular cartilage of the hip and knee joints of newborn WT and *GRN*$^{-/-}$ mice, or from 10-d-old WT and *GRN*$^{-/-}$ mice, as previously described.[35] Briefly, cartilage samples were isolated from mouse articular cartilage and human joint cartilage under sterile conditions. First, samples were dissected into tiny pieces, each with a diameter of 1 mm and thickness of 1–2 mm, and then dispensed into tissue culture flasks containing serum-free DMEM (with 25 mM HEPES, 2 mM glutamine, 100 μg/mL streptomycin, 100 IU/mL penicillin, and 2.5 μg/mL gentamicin). They were then supplemented with or without IL-1β (1 μM), PGRN (200 ng/mL), and BafA1 (0.1 μM). Following incubation, the conditioned cartilage pieces were collected for subsequent analysis. The medium was changed every two days and cultured at 37 °C and 5% CO_2 for 2 weeks. Cartilage fragments were digested in 0.25% trypsin (w/V) for 30 min, and then digested in 0.2% collagenase II (w/V) in serum-free DMEM for about 6–7 h to obtain chondrocytes. Chondrocytes were cultured in DMEM containing 10% fetal bovine serum at a density of 10^5 cells/mL. The first generation primary chondrocytes were used in the experiment.

Purification of rhPGRN

The generation of a HEK293 stable cell line expressing recombinant human PGRN protein and the purification of rhPGRN were performed as previously reported.[36,37] In short, stable cells were cultured in DMEM containing 10% FBS, 100 U/mL penicillin, 10 mg/mL streptomycin, and 1 μg/mL geneticin (G418). At 90% confluence, the complete medium was replaced with serum-free DMEM for 72 h, followed by incubation with nickel-nitrilotriacetic-agarose and purification using the ProBond™ System (Cat. No. K850-01, Life Technologies, Carlsbad, CA, USA) according to the manufacturer's instructions. The purity of recombinant PGRN was determined by SDS-PAGE and Coomassie blue staining. Protein concentration was determined using the BCA assay. The purity of recombinant PGRN was determined by SDS-PAGE and Coomassie blue staining (Fig. S2).

Cycloheximide (CHX) chase assay

6 × 10^5 cells were seeded into a 35 mm Petri dish, the medium is removed after 12 h incubated with CO_2 incubator, and a complete medium containing 10 ng/mL CHX is added. Cell lysates were collected at 0, 4, 8, 12 h for WB testing. The half-life of GAPDH mRNA is more than 24 h, [38] and we only treated cell with CHX for less than 12 h, so CHX treatment has little effect on the protein level of GAPDH.

Coimmunoprecipitation (Co-IP)

C28/I2 chondrocytes were stimulated with rapamycin for 4 or 24 h, and then cells (10^7/mL) were washed twice with sterile PBS and collected in RIPA lysis buffer containing protease inhibitors. Cartilage tissues or cell lysates were centrifuged at 12,000 rpm for 5 min at 4°C, and the protein concentration was measured using the bichorionic acid assay. Approximately 1 mL protein (1 μg/μL) from each sample was used for Co-IP. Clear supernatant (100 μL cleared supernatant or control IgG was incubated with 10 μL protein A/G agarose (Santa Cruz, USA) and primary antibody (1000 × dilution) for 24 h at 4 °C.

Histological analysis and immunohistochemistry

Knee joints were fixed in 4% PFA for 3 d and decalcified for 2 weeks in 10% w/v EDTA before dehydration and embedding in paraffin. Following embedding, 5-μm serial sections were cut, deparaffinized by xylene immersion, and rehydrated using graded ethanol prior to histological and immunohistochemical staining. Safranin O/fast green/2% hematoxylin stained sections were used to grade cartilage destruction as previously reported.[39] Sections were incubated with first antibodies, or affinity-purified monoclonal anti-COMP fragments at 4°C overnight, and a 30 min incubation with secondary antibody was performed as previous method described. Primary chondrocytes isolated from the cartilage of WT and *GRN*$^{-/-}$ mice were seeded on cover glasses in 24-well plates and treated with DMSO (control) or rapamycin (0.5 M) for 24 h. Cells were washed thrice with 1 × PBS, fixed with 4% formaldehyde for 10 min, permeabilized with 0.1% Triton X-100 in PBS for 5 min, and blocked with horse serum in PBS (1:50) for 1 h at 25°C. Next, cells were incubated with ATG5 (Novus Biologicals, NB110-53818,1:100) and ATG12 (1:100) antibodies, and then diluted in blocking buffer at 4°C overnight. The next day, cells were incubated with fluorescence-labeled secondary antibodies in blocking buffer (Abcam, ab155589, 1:200) at 37°C for 1 h. After washing thrice with PBS, tissues were mounted with 4,6-diamidino-2-phenylindole (DAPI) for 15 min. Images were taken using a confocal immunofluorescence microscope. C28/I2 and *GRN*$^{-/-}$ C28/I2 chondrocytes were also seeded on cover glasses in 24-well plates and treated with DMSO (control) or rapamycin (0.5 M) for 24 h. Then, the expression of ATG5 and ATG12 was detected under an immunofluorescence microscope, as described above. Fluorescence intensities were quantified using the ImageJ software.

Inflorescence-based of CYTO-ID® autophagy detection

Primary chondrocytes isolated from the cartilage of WT and *GRN*$^{-/-}$ mice were treated with DMSO (control) or IL-1β (1 μM) for 24 h, then stained with CYTO-ID® Green Detection Reagent and LysoTracker Red at a concentration of 300 nM was added and incubated at 37 °C for 1 h. Cells were fixed in 4% paraformaldehyde (PFA) for 10 min. Cover glasses were mounted on slides with Hoechst 33342 nuclear stain.

Histopathologic and quantificational evaluation of OA

Safranin O–stained sections were used to grade the proteoglycan content of the articular cartilage in accordance with the OARSI histology scoring system.[39] Further

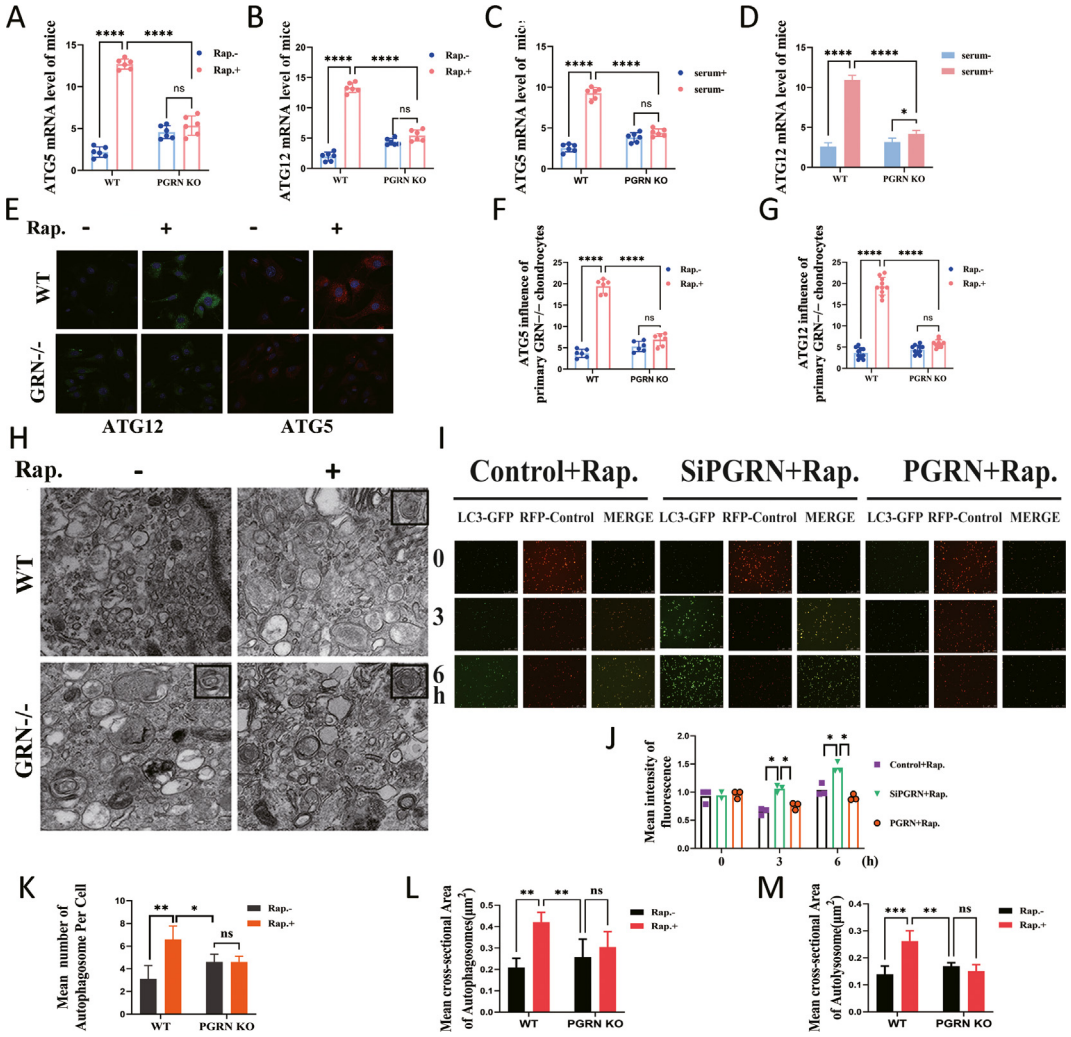

Figure 1 Autophagy is activated in murine WT and inactivated in murine *GRN*$^{-/-}$ primary chondrocytes and C28/I2 cells. mRNA levels of *ATG5* **(A, C)** and *ATG12* **(B, D)** as measured by RT-QPCR. Primary chondrocytes were isolated from the cartilage of WT and *GRN*$^{-/-}$ mice respectively, incubated and stimulated with rapamycin (0.5 μM) for 24 h (A, B) or cultured with or without serum for 24 h **(C, D)**. **(E)** Immunofluorescence assay for levels of ATG5 and ATG12 in WT and *GRN*$^{-/-}$ primary murine chondrocytes after 24 h rapamycin stimulation. Qualitative analysis of chondrocyte expressed ATG5 **(F)** and ATG12 **(G)** fluorescence intensity normalized to non-treated controls. Images were made at × 200 magnifications. **(H)** Transmission electron microscopy (TEM) analysis showing autophagosome after treatment with rapamycin for 24 h in primary chondrocytes isolated from WT and *GRN*$^{-/-}$ mice. **(I, J)** Fluorescence of autophagy dual fluorescent adenovirus was detected and quantification was analysed in C28/I2 cells treated with rapamycin (0.5 μM) for 0,3,6,12 h. The siPGRN group and PGRN group were transfected with PGRN siRNA and pcDNA3.1(-)-PGRN, respectively. Images were made at ×100 magnifications **(K—M)** Qualitative analysis of the pictures visualized under TEM. The values were normalized to the NC group. Values are means ± SD , *$P < 0.05$, **$P < 0.01$, ***$P < 0.001$, ****$P < 0.0001$; $n = 3$.

histopathologic evaluation of the stained sections was performed based on 5 random regions of interest chosen within each joint at 10× magnification. To determine whether the induction of our surgical OA model was associated with a loss of chondrocytes, articular chondrocytes were counted per unit area, and the average diameter of an articular chondrocyte was also determined. Articular cartilage thickness was measured using Adobe Photoshop 7.0 (Adobe Inc., USA). These 3 parameters were analyzed in each of the 5 randomly selected regions of interest. Values were averaged to generate a value for each mouse. Six mice were analyzed for each group. The recommended semi-quantitative scoring system was shown as Table S6.

Autophagy flux assay

C28/I2 cells and PGRN KO (*GRN*$^{-/-}$) cells were transfected with autophagy double fluorescent adenovirus for 24 h. The cells were treated with IL-1 β (1 μM) to observe the red and green fluorescence intensity at different time points. The time at the end of transfection is set as 0 h. The red fluorescence of 0 h is used to judge the transfection efficiency. With the passage of time, the red fluorescence will gradually weaken. In the process of autophagy, the green fluorescence intensity will gradually weaken. If the autophagy process is hindered, the attenuation of green fluorescence will slow down.

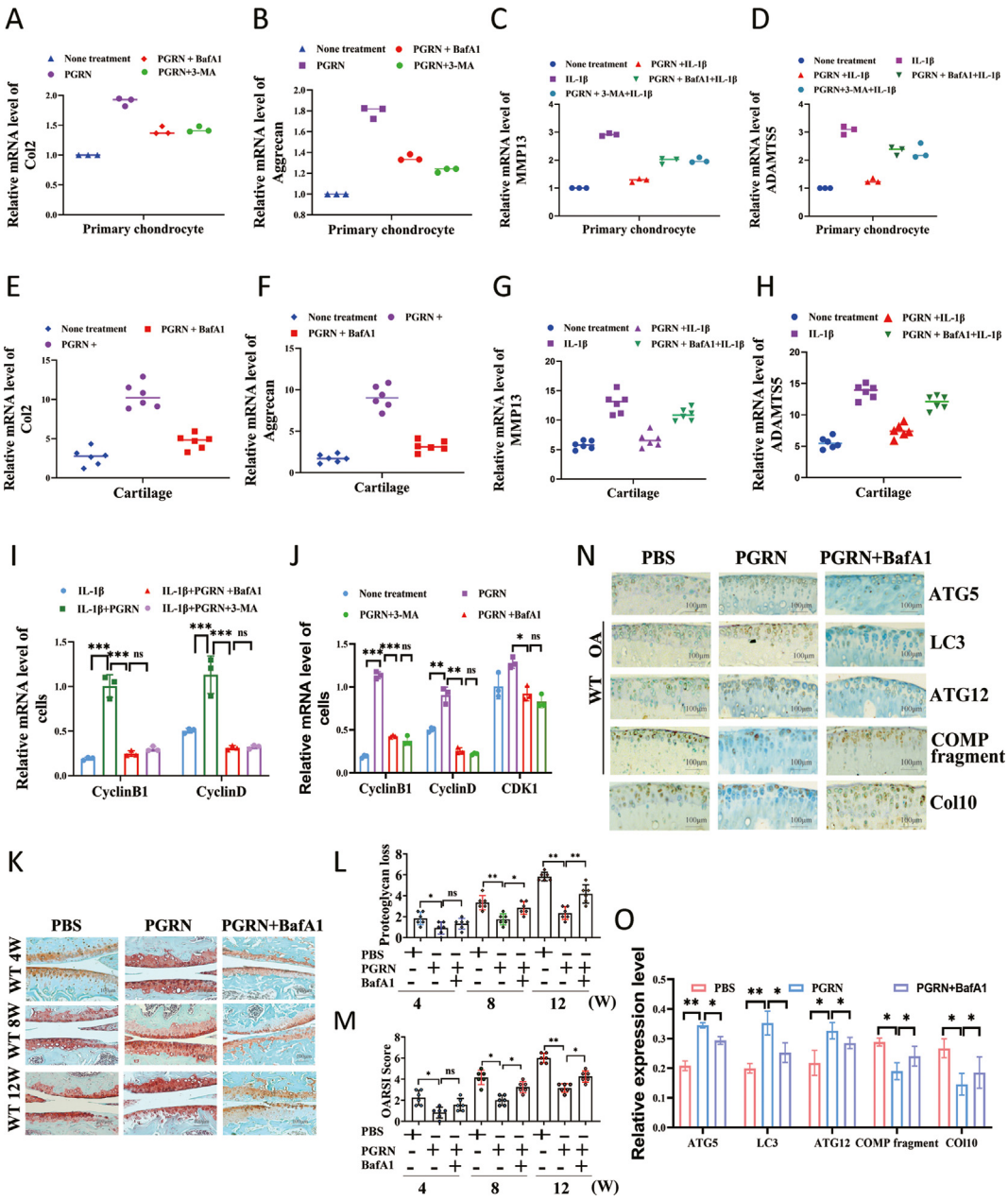

Figure 2 Autophagy influences PGRN-mediated anabolic, catabolic, proliferation effects *in vitro* and PGRN's chondroprotective effects *in vivo*. mRNA levels of *Col2* **(A)**, *Aggrecan* **(B)**, *MMP13* **(C)** and *ADAMTS5* **(D)** in primary chondrocyte as measured by real-time PCR. Primary chondrocytes were isolated from WT mice, then were incubated in presence of PGRN (200 ng/mL), PGRN + BafA1 (0.1 μM), PGRN+3-MA (5 mM), IL-1β (1 μM), IL-1β+PGRN, IL-1β+PGRN + BafA1, IL-1β+PGRN+3-MA for 24 h. mRNA levels of Col2 **(E)**, Aggrecan **(F)**, MMP13 **(G)** and ADAMTS5 **(H)** in cartilage explants isolated from osteoarthritic surgical discard tissue as measured by real-time PCR. Cartilage explants were harvested and incubated in presence of PGRN (200 ng/mL), PGRN + BafA1 (0.1 μM), IL-1β (1 μM), IL-1β+PGRN, IL-1β+PGRN + BafA1 for 7 days, followed by collection of total RNA for real-time PCR assay. **(I)** mRNA levels of *Cyclin B1*, *Cyclin D* in C28/I2 chondrocytes as measured by real-time PCR. C28/I2 chondrocytes were incubated in presence of IL-1β (1 μM), IL-1β+PGRN (200 ng/mL), IL-1β+PGRN + BafA1 (0.1 μM), IL-1β+PGRN+3-MA (5 mM) for 24 h. **(J)** mRNA levels of *Cyclin B1*, *Cyclin D*, and *CDK1* in C28/I2 chondrocytes as measured by real-time PCR. C28/I2 chondrocytes were incubated in presence of PGRN (200 ng/mL), PGRN + BafA1 (0.1 μM), PGRN+3-MA (5 mM) for 24 h. **(K)** Intra-articular injection of recombinant progranulin PGRN (6 μg) clearly protected cartilage from degeneration, however, BafA1 accelerated OA development following surgically induced OA model, assayed by Safranin O staining in WT mice. Osteoarthritis Research Society International (OARSI) score of OA **(L)** and loss of proteoglycan **(M)** based on Safranin O staining. Scale bar: 100 μm (magnification: ×100); **(N)** Immunohistochemistry staining for ATG5, LC3, ATG12, Col10 and cartilage oligomeric matrix protein (COMP) fragments. **(O)** The quantitative analysis of expression levels of ATG5, LC3, ATG12, Col10 and COMP fragments. Values are means ± SD, $n = 6$. $^{*}P < 0.05$, $^{**}P < 0.01$, $^{***}P < 0.001$.

Apoptosis and cell growth assay

C28/I2 chondrocytes were treated with DMSO (control), PGRN (200 ng/mL), and PGRN + BafA1 (0.1 μM) for 24 h. Then, plated cells were trypsinized and centrifuged at 1000 rpm for 5 min. Cells were washed by resuspending the cell pellet in cell culture medium, and then stained with a cell tracking assay using the Cyto Painter Cell Proliferation Staining Reagent - Green Fluorescence (ab176735). Fluorescence intensity, which represents cell proliferation, was measured using a flow cytometer with a 488 nm laser source. Next, C28/I2 chondrocytes were treated with DMSO (control), PGRN (200 ng/mL), PGRN + BafA1 (0.1 μM), IL-1β (1 μM), IL-1β + PGRN (200 ng/mL), and IL-1β + PGRN + BafA1 (0.1 μM) for 24 h. Next, cells were washed, trypsinized, and resuspended in 1 × PBS for flow cytometry assay on cell proliferation, as described above. In addition, C28/I2 chondrocytes were infected with Ad-RFP (control) or Ad-siATG5 for 24 h, and then washed, trypsinized, and resuspended in 1 × PBS for FCM assay or fixed with 75% alcohol to determine the distribution of cell cycle and cell apoptosis.

Statistical analysis

Statistical analysis was performed using *t*-test or one-way ANOVA or two-way ANOVA test followed by unpaired two-tailed *t*-tests. Results were presented as the mean ± standard error. $P < 0.05$, with statistically significant differences. Each point of PCR is the average of three repeated measurements.

Results

Autophagy-associated molecules were reduced in osteoarthritic cartilage

The level of PGRN and MMP13 mRNA was notably increased, whereas the mRNA levels of ATG5, ATG12, Col2 and Aggrecan were clearly downregulated in the lesion cartilage tissue compared with those from the Nonlesion cartilage of OA (Fig. S3A—F). The levels of ATG5-ATG12, ATG5, and LC3I/II proteins were decreased, whereas that of PGRN was upregulated in the lesion cartilage tissue compared with those in the Nonlesion cartilage of human OA patients. Interestingly, the levels of ATG5-ATG12, ATG5, and LC3 I/II might vary over the course of OA progression considering the different expression of these proteins in articular cartilage tissue of different patients (Fig. S3G, H).

Progranulin was required for autophagy activation in chondrocytes

The expression of ATG5 and ATG12 was notably increased in normal chondrocytes after rapamycin stimulation. However, primary *GRN*$^{-/-}$ chondrocytes exhibited no significant differences following rapamycin stimulation (Fig. 1A, B). Nutrient starvation is also known to elicit an autophagic response.[5,40] We examined the mRNA expression of ATG5 and ATG12 in cells cultured in serum-free medium for 24 h , there were notably increased at the transcriptional level in control chondrocytes, whereas *GRN*$^{-/-}$ chondrocytes exhibited no significant alterations upon nutrient starvation (Fig. 1C, D). Furthermore, immunofluorescence staining revealed that the ATG5 and ATG12 proteins also did not differ between rapamycin-treated and control *GRN*$^{-/-}$ chondrocytes (Fig. 1E—G).

Between WT and *GRN*$^{-/-}$ chondrocytes with or without rapamycin stimulation, autophagosomes were formed and present in WT chondrocytes after 24 h of rapamycin stimulation (Fig. 1H). However, no significant differences in the formation and number of autophagosome or autolysosome between untreated and rapamycin-treated *GRN*$^{-/-}$ chondrocytes (Fig. 1H, K—M). In addition, after C28/I2 cells are transfected with siPGRN, the autophagy process is blocked after rapamycin treatment for 3 h (Fig. 1I, J). Taken together, these results suggested that PGRN might be involved in autophagy activation and autophagosome formation.

We then deleted the *GRN* gene using CRISPR/Cas9 technology in C28/I2 human chondrocytes (Fig. S4A, D). Importantly, rapamycin treatment enhanced the expression of ATG5 and ATG12 in WT C28/I2 chondrocytes; however, rapamycin did not significant increase the mRNA levels of ATG5 and ATG12 in *GRN*$^{-/-}$ C28/I2 chondrocytes (Fig. S4B, E, F). In addition, rapamycin treatment also increased the level of P62, but did not show a significant effect in *GRN*$^{-/-}$ C28/I2 chondrocytes (Fig. S4C, G). Interestingly, the relative level of LC3II/ATG8 was obviously reduced in *GRN*$^{-/-}$ C28/I2 chondrocytes compared with that of in WT C28/I2 chondrocytes although rapamycin could upregulate the protein level of LC3II in *GRN*$^{-/-}$ C28/I2 chondrocytes, the degree of autophagy activated by rapamycin in *GRN*$^{-/-}$ C28/I2 chondrocytes is much lower than that of control cells (Fig. S4C, H).

In addition, a notable increase was observed in the mRNA levels of ATG5 and ATG12 in rapamycin treatment or serum-free normal chondrocytes, whereas no notable change was observed in *GRN*$^{-/-}$ C28/I2 chondrocytes following rapamycin treatment or serum starvation (Fig. S4I—L). Immunofluorescence results also demonstrated that the ATG5 and ATG12 proteins were notably increased in the normal C28/I2 chondrocytes after rapamycin stimulation. However, there was not significantly altered by rapamycin treatment in *GRN*$^{-/-}$ C28/I2 chondrocytes (Fig. S4M—O).

Progranulin was required for IL-1β-induced autophagy in chondrocytes

CYTO-ID Fluorescence staining revealed that the accumulation of autophagosomes was increased in IL-1β-stimulated murine WT primary chondrocytes compared with that of in untreated WT primary chondrocytes. Although we detected a faint autophagosomic fluorescence in IL-1β-stimulated *GRN*$^{-/-}$ murine primary chondrocytes, no significant differences were observed in autophagosome fluorescence intensity in *GRN*$^{-/-}$ chondrocytes treated with or without IL-1β. Additionally, the Lysotracker Red-labeled lysosomes were also weakened (Fig. S5A, B).

Similar trends were observed in rapamycin-treated and serum-starved chondrocytes, the mRNA levels of ATG5 and ATG12 were notably increased in control human chondrocytes after IL-1β treatment for 24 h; however, no

difference was noticed between untreated and IL-1β-stimulated *GRN*$^{-/-}$ C28/I2 chondrocytes (Fig. S5C, D).

Furthermore, fluorescence intensity in the autophagy dual fluorescent adenovirus assay showed that *GRN* knockout inhibits the attenuation of the green fluorescent protein (GFP) signal and leads to impaired autophagy flux in C28/I2. Compared with the normal C28/I2 chondrocytes (without IL-1β treatment and *GRN* gene knockout), *GRN*$^{-/-}$ C28/I2 chondrocytes have a more severe autophagic flux block after IL-1β treatment 6 h, although IL-1β can weakly activate autophagy flux. IL-1β could not completely activate the formation of autophagosomes in *GRN*$^{-/-}$ chondrocytes (Fig. S5E, F).

Autophagy was important for the protective role of progranulin in chondrocytes and osteoarthritis

We isolated primary chondrocytes from the articular cartilage of WT mice and treated them with IL-1β, PGRN, 3-MA and bafilomycin A1 (Baf A1). 3-MA is a kind of autophagy inhibitor, and Baf A1 is a typical inhibitor of the vacuole type H^+-ATPase, which prevents late-stage autophagy by inhibiting the fusion between autophagosomes and lysosomes.[41,42] Consistent with our previous findings, PGRN stimulated anabolism and inhibited the IL-1β-mediated catabolism. However, the PGRN-mediated anabolism (Fig. 2A, B) and suppression of IL-1β-induced catabolism (Fig. 2C, D) were largely attenuated after treatment with BafA1 or 3-MA. In cartilage explants isolated from human OA joint tissue, the PGRN-mediated anabolism and suppression of IL-1β-induced catabolism were largely attenuated after treatment with BafA1 (Fig. 2E—H). Furthermore, we found that the PGRN-induced cell proliferation was restrained in BafA1-treated and 3-MA-treated chondrocytes compared with that of controls (Fig. 2I, J).

Intra-articular injection of PGRN dramatically protected the cartilage from degeneration in the surgically induced OA model, whereas intra-articular injection of the autophagy inhibitor, BafA1, clearly suppressed the protective effect of PGRN and significantly abolished the PGRN-induced suppression of catabolism. We evaluated all safranin O-stained sections in accordance with OARSI scoring system.[39] We respectively observed a significant protective effect of PGRN on proteoglycan content and cartilage homeostasis in OA. Importantly, these protective effects of PGRN were abolished after treatment with Baf A1 (Fig. 2K—M).

Immunohistochemistry staining revealed that PGRN treatment was associated with reduced staining for Col X and COMP fragments, whereas simultaneous treatment with PGRN and Baf A1 induced the increased expression of these chondrocyte hypertrophy and cartilage degradation markers alongside the downregulation of autophagy markers (ATG5, LC3II, and ATG12) (Fig. 2N, O). Taken together, these results demonstrated that PGRN-regulated autophagy contributes to the chondroprotective effect of PGRN against OA.

Progranulin interacted with the ATG5-ATG12 conjugate in chondrocytes

Compared with after rapamycin stimulation for 4 h, the expression of PGRN, ATG5, ATG5-ATG12, P62 and LC3II increased with the prolong of the rapamycin treatment (Fig. 3A, B). Focusing at the role of PGRN as a chaperone, we analyzed the structures of PGRN and some important autophagy-related proteins using the Protein Data Bank (PDBePISA http://www.ebi.ac.uk/pdbe/pisa/pistart.html) to predict the interactions between PGRN and these key autophagy markers. Interestingly, our predicted protein interaction assessment prompted us to determine whether PGRN interacts with ATG5 or ATG5-ATG12 in chondrocytes. We used immunofluorescence staining to further supporting the interaction of PGRN and ATG5-ATG12 (Fig. 3C). Next, we examined ATG5 or ATG12 protein half-life by blocking denovo synthesis with CHX and anti-ATG5 or ATG12 antibody (Fig. 3D, E). Cells were treated with CHX and lysed after 0, 4,8 and 12 h. Protein levels in PGRN KO (*GRN*$^{-/-}$) cells rapidly decreased after addition of CHX (Fig. 3H, I). Similarly, after transfection with Ad-siATG5 or siATG12, PGRN protein levels in cells rapidly decreased after addition of CHX (Fig. 3F, G, J, K). These data indicate PGRN affects ATG5 or ATG12 stability each other. Coimmunoprecipitation assay results revealed that PGRN bound to the ATG5-ATG12 conjugate in the primary chondrocytes isolated from the cartilage tissues from wild-type mice and the cartilage tissue from OA patient (Fig. 3L, M). Then transfect siPGRN or Ad-siATG5 or siATG12 in C28/I2 cells, and together with *GRN*$^{-/-}$ or *ATG5* KO cells to use Co-IP detect the binding of related proteins (Fig. 3N). These results further confirmed that PGRN can bind to ATG5 and ATG12 in chondrocyte.

ATG5 was required for the anabolic and anticatabolic effects of PGRN *in vitro*

Western blotting revealed the effective knockdown of ATG5 or ATG12 and the blocking of the conversion of endogenous LC3 (LC3II/ATG8) concurrent with the enhanced expression of P62, cleaved Caspase3, and Caspase12 in chondrocytes following exposure to ATG5 Ad-siRNA or ATG12 siRNA (Fig. 4A, D). Flow cytometry results also revealed the reduced proliferation and increased apoptosis of siATG5-infected chondrocytes (Fig. 4B, C, E, F).

To further illustrate the importance of ATG5 in the chondroprotective effects of PGRN, we generated *ATG5*$^{-/-}$ C28/I2 chondrocytes using the CRISPR/cas9 technique. We treated *ATG5*$^{-/-}$ and WT chondrocytes with or without PGRN and then subjected them to transcriptional analysis. The PGRN-mediated stimulation of chondrocyte anabolism and inhibition of IL-1β-induced catabolism were largely abolished in *ATG5*$^{-/-}$ chondrocytes compared with normal chondrocyte (Fig. 4G—J). In contrast, introduction of an ATG5-overexpressing adenovirus (Ad*ATG5*) rescued the above effects in *ATG5*$^{-/-}$ chondrocytes (Fig. 4K—N). Cumulatively, the pro-anabolic and anticatabolic effects of PGRN in chondrocytes are dependent upon the expression of ATG5.

Determination of the binding domains of PGRN with ATG5 and ATG12

As PGRN could affect the expression of ATG5 and ATG12, and there have an interaction between PGRN, ATG5 and ATG12 (Fig. 3L—N), we sought to determine which binding

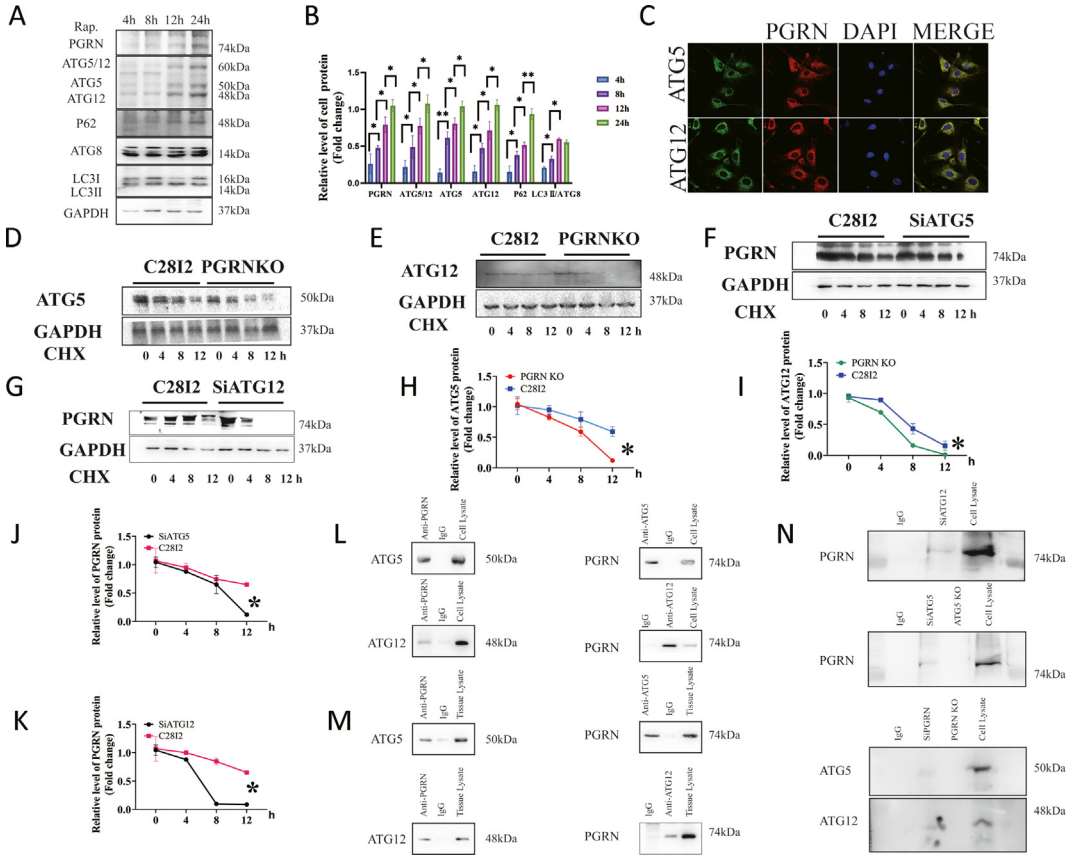

Figure 3 Assay on the co-localization and interaction between PGRN and ATG5-ATG12 conjugate in chondrocyte. **(A)** Western blot analysis showing the expression of ATG5, ATG12, ATG5-ATG12, P62, ATG8, LC3I/II and PGRN in C28/I2 treated rapamycin for 4, 8, 12, 24 h. **(B)** Qualitative analysis of the expression of PGRN, ATG5, ATG12, ATG5-ATG12, P62 and LC3II/ATG8 were normalized to GAPDH. **(C)** Immunofluorescence staining showing the co-localization of PGRN and ATG5, PGRN and ATG12. Images were made at ×200 magnifications. **(D—G)** ATG5 or ATG12 or PGRN degradation were analyzed by cycloheximide chase assay. **(H—K)** Representative images and quantitative data for ATG5 or ATG12 or PGRN protein level are shown. **(L)** Primary chondrocytes were isolated from the cartilage of wide type mice, followed by collection of cell lysate for Co-IP assay. Cell lysate was immunoprecipitated with PGRN antibody and probed with ATG5, ATG12 antibody respectively. Conversely, IP was performed with ATG12 antibody and probed with PGRN antibody. **(M)** Cartilage tissue were isolated from OA patient, followed by collection of tissue lysate for Co-IP assay. The method is the same as before. **(N)** C28/I2 cells were transfected with siPGRN, Ad-siATG5 and siATG12, respectively, Co-IP was done with ATG5 KO and/or PGRN KO cells. Values are means ± SD. $^{*}P < 0.05$, $^{**}P < 0.01$.

site of PGRN bound to ATG5 or ATG12. C-and N-terminal deletion mutants of PGRN were constructed (Fig. S5A, B; Fig. S6), then constructs expressing GFP-tagged PGRN and its deletion mutants and MYC-tagged ATG5 or ATG12 were co-transfected in 293 cells. The western blot result indicated that PGRN and all the deletion mutants were expressed after transfection as detected with a GFP antibody (Fig. 5C, D), and ATG5 or ATG12 can also be overexpressed in 293 cells normally (Fig. 5E). Furthermore, the cell lysate was next immunoprecipitated with MYC-tag antibody or GFP antibody and probed by GFP antibody or MYC antibody. As shown in Figure 5F—H, after over expression of ATG5, there is a binding between ATG5 and PGRN full length and all PGRN deletion mutants from the ND1 to ND7, which means that GRN E is essential for binding ATG5; meanwhile, there is also binding between ATG5 and PGRN full length and all of PGRN deletion mutants from the CD1 to CD6, and the binding was lost in CD7, this indicates that the G domain of GRN is one binding motif.

After overexpression of ATG12, ND7 showed binding, suggesting that GRN E is important. In addition, there is also binding between ATG12 and PGRN full length and all PGRN deletion mutants from the CD1 to CD6, and the binding was absent in CD7, this implies that GRN G is one of binding motif between PGRN and ATG12. Furthermore, the combination of CD5 and ATG12 is stronger than that of CD6, which indicates that GRN F may play an important role in the process of PGRN and ATG12 binding.

Our results implies ATG5 and ATG12 can both binding PGRN through GRN E, we further investigated the binding motif important for ATG5-ATG12 interaction within GRN E. 293 cells were transfected with serial deletions from Δ1 to Δ 6 in GRN E and its linker region (Fig. 5I) and Co-IP was performed; results revealed that the Δ2 (deletion of aa523—534),Δ5 (aa574-590) and Δ6 (deletion of aa591—593) fragment almost abrogated binding, indicating that the aa523—534, aa574-590 and aa591-593 sequence are both critical for the binding between PGRN and ATG5-ATG12 (Fig. 5J).

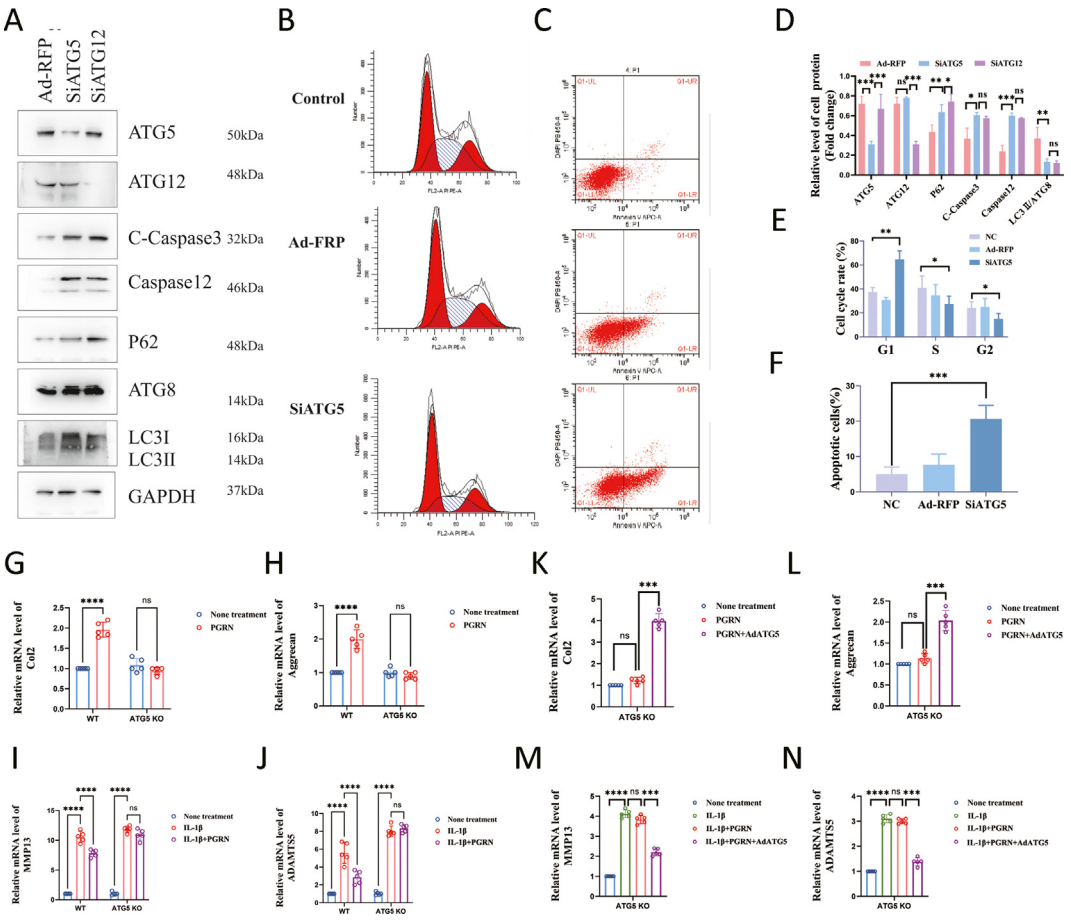

Figure 4 The ATG12-ATG5 conjugate is important for the PGRN mediated chondroprotective effect. **(A, D)** Expressions and qualitative analysis of ATG5, ATG12, cleaved caspase3, caspase12, P62, ATG8, LC3I/II in chondrocytes infected by siATG5 and siATG12. GAPDH is an internal control. **(B, E)** Flow cytometry analysis with Annexin V-PI staining was performed to evaluate the percentage of S phase, G1 phase and G2 phase in siATG5-infected C28/I2 chondrocytes. **(C, F)** Dot plots of flow cytometry analysis with Annexin V-PI staining were performed to evaluate the percentage of apoptotic cells in siATG5-infected C28/I2 chondrocytes. mRNA level of Col2 **(G)**, Aggrecan **(H)** in WT and *ATG5*$^{-/-}$ chondrocytes with or without PGRN (200 ng/mL). IL-1β-induced (1 μM) mRNA level of MMP13 **(I)** and ADAMTS5 **(J)** in WT and *ATG5*$^{-/-}$ chondrocytes with or without PGRN recombinant protein. mRNA level of *Col2* **(K)** and *Aggrecan* **(L)** in *ATG5*$^{-/-}$ chondrocytes with or without PGRN (200 ng/mL) and Ad-ATG5. IL-1β-induced (1 μM) mRNA level of *MMP13* **(M)** and *ADAMTS5* **(N)** in *ATG5*$^{-/-}$ chondrocytes with or without PGRN recombinant protein and Ad-ATG5. Values are means ± SD, *$P < 0.05$, **$P < 0.01$, ***$P < 0.001$, ****$P < 0.0001$.

Discussion

OA is a common degenerative condition of the joints characterized by the progressive degradation of cartilage. Autophagy, which is essential for cell survival and function, is a well-defined self-digestion process, in which cytoplasmic contents are delivered to lysosomes for recycling.[9,41] Furthermore, autophagy has been implicated in the retardation of aging and age-associated diseases, such as osteoarthritis, through the modulation of cell homeostasis and cell death. Reduced autophagic activity has also been reported to be accompanied by increased apoptosis and enhanced rate of chondrocyte damage and cartilage degeneration, with varied levels of autophagy activation correlated with OA grade.[43,44]

Zhao et al previously found that PGRN regulated chondrocyte metabolism, and intra-articular injection of recombinant PGRN attenuated OA-like phenotypes and protected against OA progression in surgically-induced OA models.[4] Herein, PGRN is proved to be critical for rapamycin- and serum free-induced chondrocyte autophagy activation. More than 30 autophagy-related genes control autophagy activation. Among them, ATG5 and ATG12 are two essential autophagy proteins that are involved in autophagosome formation. Microtubule-associated protein 1 light chain 3 (LC3), including LC3 I and LC3 II, governs autophagosome elongation,[45–47] ATG8 is equivalent to LC3, which is just a different name for the same protein in different systems.[29]

The IL-1 family of catabolic cytokines is regarded as a principal factor of joint damage in OA and underlying degradation of aggrecan and collagen.[48,49] Autophagy regulates and is regulated by a wide range of proinflammatory cytokines, with IL-1 emerging as a reliable inducer of

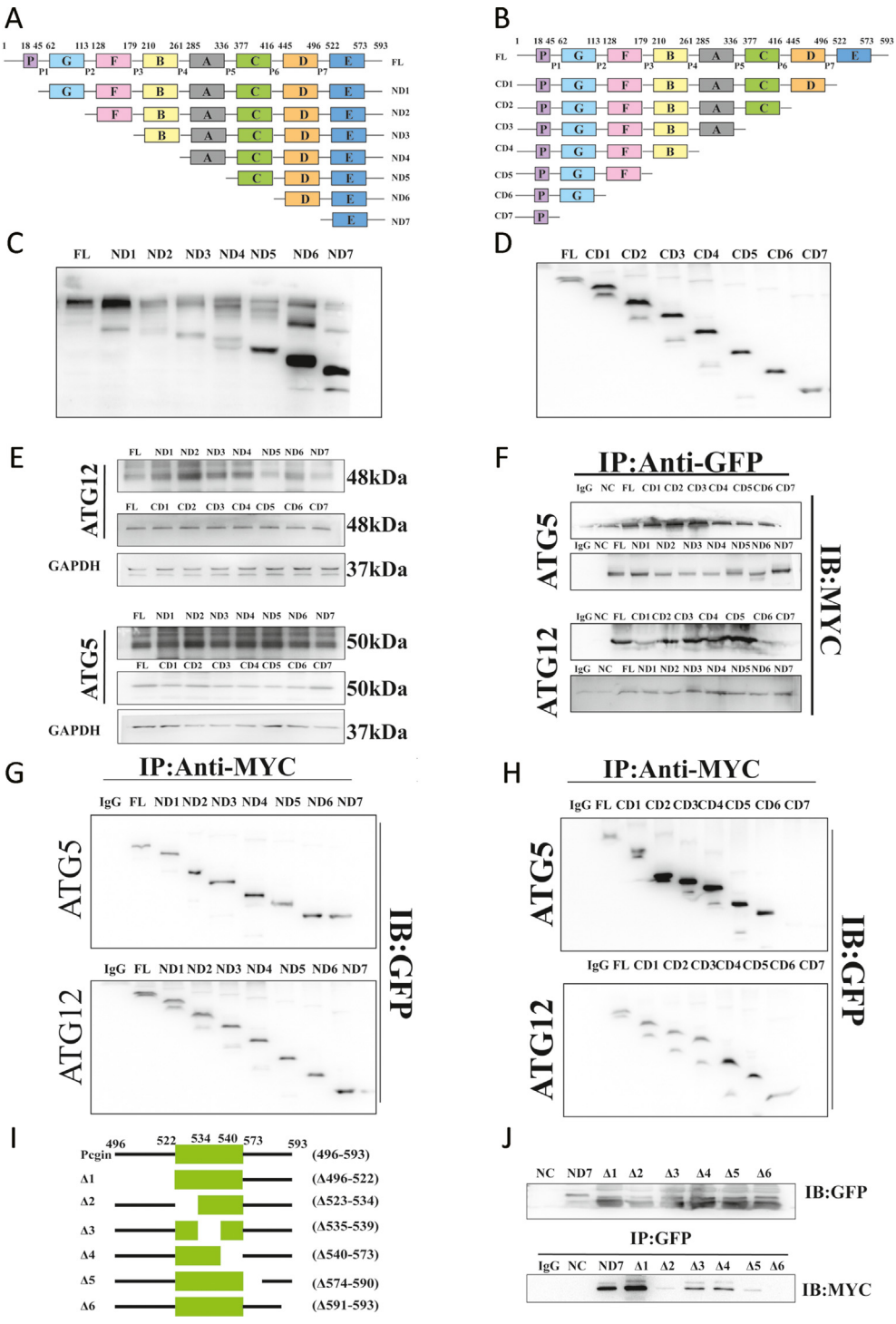

Figure 5 PGRN binds to ATG5 and ATG12 through GRN G, E and F. **(A)** Scheme of constructs encoding serial GFP-tagged N-terminal deletion mutants of PGRN. **(B)** Scheme of constructs encoding serial GFP-tagged C-terminal deletion mutants of PGRN. **(C)** Expressions of GFP-tagged N-terminal deletion PGRN fragments, examined with anti-GFP antibody. **(D)** Expressions of GFP-tagged C-terminal deletion PGRN fragments, examined with anti-GFP antibody. **(E)** The overexpression of ATG5 and ATG12 at the N-terminus and C-terminus, respectively. **(F)** Co-IP assay. The cell lysates were immunoprecipitated with GFP antibody. The complexes were probed with anti-MYC antibody. **(G)** Co-IP assay. The cell lysates were immunoprecipitated with MYC antibody. The complexes were probed with anti-GFP antibody at the N-terminus. **(H)** Co-IP assay. The cell lysates were immunoprecipitated with MYC antibody. The complexes were probed with anti-GFP antibody at the C-terminus. **(I)** The construction of Pcgin mutants. **(J)** Expression (top) of Pcgin and its mutants after transfection. The cell lysate was immunoprecipitated with GFP antibody and probed with MYC antibody (bottom).

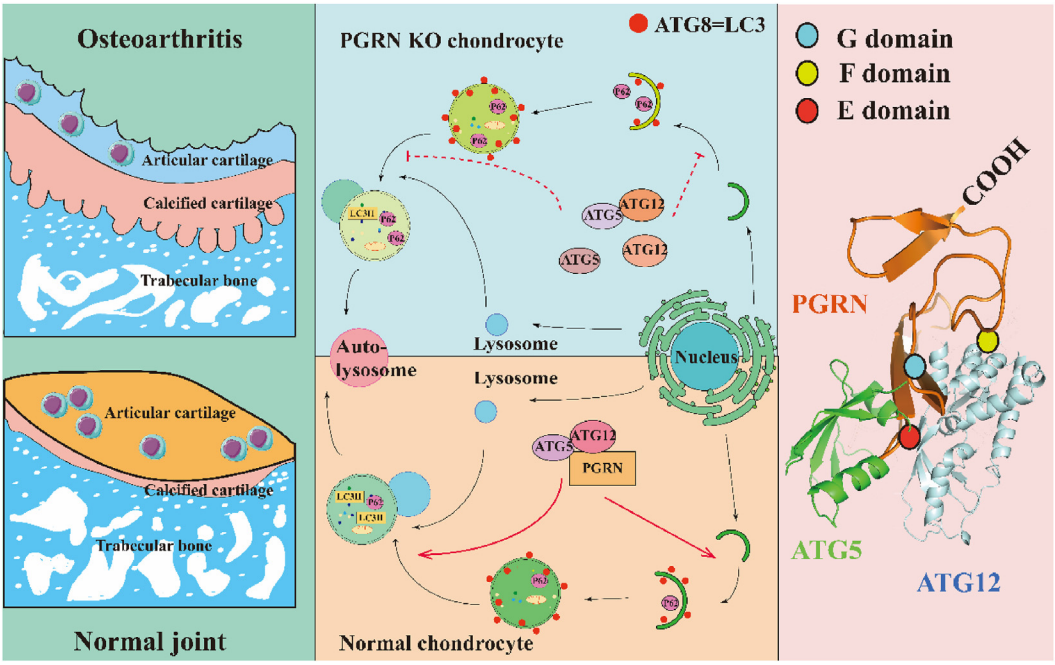

Figure 6 The pattern diagram of PGRN involvement in autophagy in chondrocyte. In the pathological process of osteoarthritis, autophagy activity is weakened due to the loss of PGRN, and insufficient binding of PGRN and ATG5-ATG12 complex affects the initiation, elongation, maturation and degradation of autophagy. The combination of PGRN and ATG5 is through G and E domains, and in addition to G and E domains, F domain also plays a key role in the combination of PGRN and ATG12.

autophagy.[50] PGRN is involved in IL-1β-induced autophagosome formation and the fusion between autophagosome with lysosome.

Furthermore, the PGRN-mediated anabolism and suppression of IL-1β-induced catabolism were largely abolished in the presence of BafA1 and 3-MA. Intra-articular injection of BafA1 dramatically abolished the protective effects of PGRN against OA (Fig. 2). Collectively, autophagy is vital for the protective role of PGRN in human chondrocytes and murine surgically-induced OA. PGRN deficiency led to the impairment of autophagy activation or autophagy flux by reducing the fusion between autophagosomes and lysosomes in chondrocytes and in an OA mouse model. In OA chondrocytes, the mRNA and protein levels of ATG5—ATG12, and ATG5 were markedly downregulated, whereas the level of PGRN was upregulated. Notably, PGRN-deficient primary chondrocytes exhibited no significant difference in the mRNA and protein levels of PGRN, ATG5—ATG12, or ATG5 upon rapamycin- or IL-1β-induced autophagy. The correlating trends of the reduced expression of autophagy markers observed in OA chondrocytes and PGRN-deficient cells, together with the responsivity of the latter to autophagy-activating stimuli led us to deduce that PGRN functions closely related with autophagy under homeostatic conditions and that this function might be disrupted in OA.

More importantly, genetic and *in vitro* studies have indicated that the level of the ATG12—ATG5 conjugate is essential for autophagic activity.[51] PGRN deficiency results in reduced expression of PGRN and ATG5, reduction of PGRN-ATG5 and PGRN-ATG5-ATG12 interactions, and impairment of autophagy activation. These findings suggested that PGRN-mediated chondroprotection depends on the adequate interaction between PGRN and the ATG12—ATG5 conjugate (Fig. 3). In cartilage, chondrocyte autophagy is necessary for maintaining homeostasis, survival of chondrocytes, and maintaining cartilage integrity.[52] The transition from autophagy to apoptosis is known to play a key role in the process of OA. Herein, PGRN-mediated autophagy is crucial for its chondroprotective effect in osteoarthritis. In particularly, this chondroprotective effect relies on the ATG5-ATG12 conjugate, and it is achieved by affecting the proliferation and apoptosis of chondrocytes (Fig. 4).

Interestingly, PGRN binds to ATG5 and ATG12 with different binding sites. We identified that PGRN binds to ATG5 through GRN G and E; and PGRN binds to ATG12 through GRN G, E and F.GRN E is a major protein—protein interaction domain for PGRN, as it has been shown to bind to other proteins.[53]CD6, the C-terminal deletion of PGRN, binds to ATG5 and ATG12 (Fig. 5).

ATG12 docks onto ATG5 through conserved residues. ATG12 and ATG5 are oriented such that other conserved residues on each molecule, including the conjugation junction, form a continuous surface patch.[54] As summarized in the model of Figure 6, PGRN is involved in the autophagy process through binding with ATG5-ATG12 complex and its chondroprotective role in OA is dependent on autophagy. The binding domains of PGRN and ATG5 or ATG12 are not exactly same, this may be due to that PGRN is folded and part of it extends into the gap between the bonding surface of ATG5 and ATG12, so that the two shared E and G domain, and the F domain located in the other half of the folded PGRN may bind to ATG12. ATG12 is reported to be irreversibly conjugated to ATG5,[55] The combination of PGRN and ATG5-ATG12 determines the function of PGRN in

autophagy and chondroprotective effect. In this paper, C28/I2 cells are mainly used to explore the association between chondrocytes and autophagy under OA conditions. C28/I2 cells can be transmitted more generations and are easier to culture, but the disadvantage is that with the increase of culture generations, due to the lack of normal extracellular matrix (ECM), isolated cells may have phenotypic changes, thus limiting the study of intercellular and cell-to-ECM interactions. Therefore, we also supplemented primary chondrocytes as well as mouse knee explants to avoid the shortage of C28/I2 cell experiments. OA is a multifactorial disease, although the evidence for a role of IL-1β in OA is well established,[56] it is not comprehensive enough.

In conclusion, our findings indicated that autophagy is a novel therapeutic target for PGRN-associated diseases and highlighted the emerging theme of defective autophagy in cartilage degenerative diseases.

Author contributions

All authors contributed to the study conception and design. Experiments were designed by Fengjin Guo, Yiming Pan and Yuyou Yang. Experiments were carried out by Yiming Pan, Yuyou Yang, Rong Jiang, Mengtian Fan, Li Li, Menglin Xian, Nana Geng, Naibo Feng, Wei Zheng, Lin Deng, and Fengmei Zhang. Cheng Chen and Biao Kuang provided the cartilage tissues of OA patients. Data were analyzed by Yiming Pan, Yuyou Yang, Xiaoli Li, and Fengjin Guo.
Prof. Fengjin Guo designed the manuscript and had full access to all of the data in the study and takes responsibility for the integrity of the data and the accuracy of the data analysis. All authors have given approval to the final version of the manuscript.

Conflict of interests

The authors have no relevant financial or non-financial interests to disclose.

Funding

This work was supported by the National Natural Science Foundation of China (No. 81672209); Chongqing Science and Technology Bureau (No. cstc2020jcyj-msxmX0175), China; Chongqing Human Resources and Social Security Bureau (No. 2018-389), China.

Data availability

All data is available in the main text or the Supplementary Materials.

Ethics declaration

This study was performed in line with the principles of the Declaration of Helsinki. Approval was granted by the Ethics Committee of ChongQing Medical University (March 23, 2021).

Acknowledgements

The authors would like to thank Prof. Chuanju Liu (Department of Orthopaedic Surgery and Cell Biology, New York University School of Medicine) for giving us some good suggestions on the manuscript and donating the plasmids and cell lines used in this experiment.

Appendix A. Supplementary data

Supplementary data to this article can be found online at https://doi.org/10.1016/j.gendis.2022.05.031.

References

1. Wei JL, Fu W, Ding YJ, et al. Progranulin derivative Atsttrin protects against early osteoarthritis in mouse and rat models. *Arthritis Res Ther*. 2017;19(1):280.
2. Xia Q, Zhu S, Wu Y, et al. Intra-articular transplantation of atsttrin-transduced mesenchymal stem cells ameliorate osteoarthritis development. *Stem Cells Transl Med*. 2015;4(5):523—531.
3. Millerand M, Berenbaum F, Jacques C. Danger signals and inflammaging in osteoarthritis. *Clin Exp Rheumatol*. 2019;37 Suppl 120(5):48—56.
4. Hunter DJ, Bierma-Zeinstra S. Osteoarthritis. *Lancet*. 2019;393(10182):1745—1759.
5. Lotz MK, Caramés B. Autophagy and cartilage homeostasis mechanisms in joint health, aging and OA. *Nat Rev Rheumatol*. 2011;7(10):579—587.
6. Lin TY, Chan HH, Chen SH, et al. BIRC5/Survivin is a novel ATG12-ATG5 conjugate interactor and an autophagy-induced DNA damage suppressor in human cancer and mouse embryonic fibroblast cells. *Autophagy*. 2020;16(7):1296—1313.
7. Caramés B, Taniguchi N, Otsuki S, Blanco FJ, Lotz M. Autophagy is a protective mechanism in normal cartilage, and its aging-related loss is linked with cell death and osteoarthritis. *Arthritis Rheum*. 2010;62(3):791—801.
8. Caramés B, Olmer M, Kiosses WB, Lotz MK. The relationship of autophagy defects to cartilage damage during joint aging in a mouse model. *Arthritis Rheumatol*. 2015;67(6):1568—1576.
9. Loeser RF, Collins JA, Diekman BO. Ageing and the pathogenesis of osteoarthritis. *Nat Rev Rheumatol*. 2016;12(7):412—420.
10. Guo F, Lai Y, Tian Q, Lin EA, Kong L, Liu C. Granulin-epithelin precursor binds directly to ADAMTS-7 and ADAMTS-12 and inhibits their degradation of cartilage oligomeric matrix protein. *Arthritis Rheum*. 2010;62(7):2023—2036.
11. Wei J, Hettinghouse A, Liu C. The role of progranulin in arthritis. *Ann N Y Acad Sci*. 2016;1383(1):5—20.
12. He Z, Ong CH, Halper J, Bateman A. Progranulin is a mediator of the wound response. *Nat Med*. 2003;9(2):225—229.
13. Zhao YP, Tian QY, Frenkel S, Liu CJ. The promotion of bone healing by progranulin, a downstream molecule of BMP-2, through interacting with TNF/TNFR signaling. *Biomaterials*. 2013;34(27):6412—6421.
14. Feng JQ, Guo FJ, Jiang BC, et al. Granulin epithelin precursor: a bone morphogenic protein 2-inducible growth factor that activates Erk1/2 signaling and JunB transcription factor in chondrogenesis. *FASEB J*. 2010;24(6):1879—1892.
15. Zhu J, Nathan C, Jin W, et al. Conversion of proepithelin to epithelins: roles of SLPI and elastase in host defense and wound repair. *Cell*. 2002;111(6):867—878.
16. Shlopov BV, Stuart JM, Gumanovskaya ML, Hasty KA. Regulation of cartilage collagenase by doxycycline. *J Rheumatol*. 2001;28(4):835—842.

17. Chou CH, Jain V, Gibson J, et al. Synovial cell cross-talk with cartilage plays a major role in the pathogenesis of osteoarthritis. *Sci Rep*. 2020;10(1):10868.
18. Chan MWY, Gomez-Aristizábal A, Mahomed N, Gandhi R, Viswanathan S. A tool for evaluating novel osteoarthritis therapies using multivariate analyses of human cartilage-synovium explant co-culture. *Osteoarthritis Cartilage*. 2022; 30(1):147—159.
19. Fernandes AM, Herlofsen SR, Karlsen TA, Küchler AM, Fløisand Y, Brinchmann JE. Similar properties of chondrocytes from osteoarthritis joints and mesenchymal stem cells from healthy donors for tissue engineering of articular cartilage. *PLoS One*. 2013;8(5):e62994.
20. Li M, Liu Y, Xia F, et al. Progranulin is required for proper ER stress response and inhibits ER stress-mediated apoptosis through TNFR2. *Cell Signal*. 2014;26(7):1539—1548.
21. Tang W, Lu Y, Tian QY, et al. The growth factor progranulin binds to TNF receptors and is therapeutic against inflammatory arthritis in mice. *Science*. 2011;332(6028):478—484.
22. Culley KL, Dragomir CL, Chang J, et al. Mouse models of osteoarthritis: surgical model of posttraumatic osteoarthritis induced by destabilization of the medial meniscus. *Methods Mol Biol*. 2015;1226:143—173.
23. Kuang L, Wu J, Su N, et al. FGFR3 deficiency enhances CXCL12-dependent chemotaxis of macrophages via upregulating CXCR7 and aggravates joint destruction in mice. *Ann Rheum Dis*. 2020; 79(1):112—122.
24. Lee KI, Choi S, Matsuzaki T, et al. FOXO1 and FOXO3 transcription factors have unique functions in meniscus development and homeostasis during aging and osteoarthritis. *Proc Natl Acad Sci U S A*. 2020;117(6):3135—3143.
25. Glasson SS, Blanchet TJ, Morris EA. The surgical destabilization of the medial meniscus (DMM) model of osteoarthritis in the 129/SvEv mouse. *Osteoarthritis Cartilage*. 2007;15(9): 1061—1069.
26. Bao J, Chen Z, Xu L, Wu L, Xiong Y. Rapamycin protects chondrocytes against IL-18-induced apoptosis and ameliorates rat osteoarthritis. *Aging (Albany NY)*. 2020;12(6):5152—5167.
27. Zhang T, Liu J, Zheng X, Zhang B, Xia C. Different roles of Akt and mechanistic target of rapamycin in serum-dependent chondroprotection of human osteoarthritic chondrocytes. *Int J Mol Med*. 2018;41(2):977—984.
28. Tang Y, Mo Y, Xin D, Zeng L, Yue Z, Xu C. β-ecdysterone alleviates osteoarthritis by activating autophagy in chondrocytes through regulating PI3K/AKT/mTOR signal pathway. *Am J Transl Res*. 2020;12(11):7174—7186.
29. Klionsky DJ, Abdalla FC, Abeliovich H, et al. Guidelines for the use and interpretation of assays for monitoring autophagy. *Autophagy*. 2012;8(4):445—544.
30. Zhang F, Wen Y, Guo X. CRISPR/Cas9 for genome editing: progress, implications and challenges. *Hum Mol Genet*. 2014; 23(R1):R40—R46.
31. Savić N, Schwank G. Advances in therapeutic CRISPR/Cas9 genome editing. *Transl Res*. 2016;168:15—21.
32. Moo EK, Osman NA, Pingguan-Murphy B. The metabolic dynamics of cartilage explants over a long-term culture period. *Clinics (Sao Paulo)*. 2011;66(8):1431—1436.
33. Haltmayer E, Ribitsch I, Gabner S, et al. Co-culture of osteochondral explants and synovial membrane as in vitro model for osteoarthritis. *PLoS One*. 2019;14(4):e0214709.
34. Geurts J, Jurić D, Müller M, Schären S, Netzer C. Novel ex vivo human osteochondral explant model of knee and spine osteoarthritis enables assessment of inflammatory and drug treatment responses. *Int J Mol Sci*. 2018;19(5).
35. Guo FJ, Xiong Z, Lu X, Ye M, Han X, Jiang R. ATF6 upregulates XBP1S and inhibits ER stress-mediated apoptosis in osteoarthritis cartilage. *Cell Signal*. 2014;26(2):332—342.
36. Lang I, Füllsack S, Wajant H. Lack of evidence for a direct interaction of progranulin and tumor necrosis factor receptor-1 and tumor necrosis factor receptor-2 from cellular binding studies. *Front Immunol*. 2018;9:793.
37. Zhao YP, Liu B, Tian QY, Wei JL, Richbourgh B, Liu CJ. Progranulin protects against osteoarthritis through interacting with TNF-α and β-Catenin signalling. *Ann Rheum Dis*. 2015; 74(12):2244—2253.
38. Lekas P, Tin KL, Lee C, Prokipcak RD. The human cytochrome P450 1A1 mRNA is rapidly degraded in HepG2 cells. *Arch Biochem Biophys*. 2000;384(2):311—318.
39. Glasson SS, Chambers MG, Van Den Berg WB, Little CB. The OARSI histopathology initiative - recommendations for histological assessments of osteoarthritis in the mouse. *Osteoarthritis Cartilage*. 2010;18(Suppl 3):S17—S23.
40. Liu R, Chen Y, Fu W, et al. Fexofenadine inhibits TNF signaling through targeting to cytosolic phospholipase A2 and is therapeutic against inflammatory arthritis. *Ann Rheum Dis*. 2019; 78(11):1524—1535.
41. Harris J, Lang T, Thomas JPW, Sukkar MB, Nabar NR, Kehrl JH. Autophagy and inflammasomes. *Mol Immunol*. 2017;86:10—15.
42. Yang H, Wen Y, Zhang M, et al. MTORC1 coordinates the autophagy and apoptosis signaling in articular chondrocytes in osteoarthritic temporomandibular joint. *Autophagy*. 2020; 16(2):271—288.
43. Bateman A, Cheung ST, Bennett HPJ. A brief overview of progranulin in health and disease. *Methods Mol Biol*. 2018;1806: 3—15.
44. Harris J. Autophagy and cytokines. *Cytokine*. 2011;56(2): 140—144.
45. Schroeppel JP, Crist JD, Anderson HC, Wang J. Molecular regulation of articular chondrocyte function and its significance in osteoarthritis. *Histol Histopathol*. 2011;26(3): 377—394.
46. Berenbaum F. Proinflammatory cytokines, prostaglandins, and the chondrocyte: mechanisms of intracellular activation. *Joint Bone Spine*. 2000;67(6):561—564.
47. Kawaguchi H. Endochondral ossification signals in cartilage degradation during osteoarthritis progression in experimental mouse models. *Mol Cells*. 2008;25(1):1—6.
48. Ravikumar B, Sarkar S, Davies JE, et al. Regulation of mammalian autophagy in physiology and pathophysiology. *Physiol Rev*. 2010;90(4):1383—1435.
49. Alvarez-García O, García-López E, Loredo V, et al. Rapamycin induces growth retardation by disrupting angiogenesis in the growth plate. *Kidney Int*. 2010;78(6):561—568.
50. Jenei-Lanzl Z, Meurer A, Zaucke F. Interleukin-1β signaling in osteoarthritis - chondrocytes in focus. *Cell Signal*. 2019;53: 212—223.
51. D'Adamo S, Cetrullo S, Minguzzi M, Silvestri Y, Borzì RM, Flamigni F. MicroRNAs and autophagy: fine players in the control of chondrocyte homeostatic activities in osteoarthritis. *Oxid Med Cell Longev*. 2017;2017:3720128.
52. Chun Y, Kim J. Autophagy: an essential degradation program for cellular homeostasis and life. *Cells*. 2018;7(12).
53. Chen Y, Jian J, Hettinghouse A, et al. Progranulin associates with hexosaminidase A and ameliorates GM2 ganglioside accumulation and lysosomal storage in Tay-Sachs disease. *J Mol Med (Berl)*. 2018;96(12):1359—1373.
54. Otomo C, Metlagel Z, Takaesu G, Otomo T. Structure of the human ATG12∼ATG5 conjugate required for LC3 lipidation in autophagy. *Nat Struct Mol Biol*. 2013;20(1):59—66.
55. Parzych KR, Klionsky DJ. An overview of autophagy: morphology, mechanism, and regulation. *Antioxidants Redox Signal*. 2014;20(3):460—473.
56. Johnson CI, Argyle DJ, Clements DN. In vitro models for the study of osteoarthritis. *Vet J*. 2016;209:40—49.